www.trjfas.org
ISSN 1303-2712
Turkish Journal of Fisheries and Aquatic Sciences 18:1409-1420(2018) DOI: 10.4194/1303-2712-v18_12_09

RESEARCH PAPER

Identification, Characterization and Expression Patterns of a *Caspase-14* Gene from the Chinese Soft-Shelled Turtle *Pelodiscus sinensis* under Immune Challenge

Bin Sun[1], Peng Li[1,3,*], Jie Yan[1,*], Siting Wang[1], Hong Li[1], Lian Chen[2], Yanfu Qu[1], Kaiya Zhou[1]

[1] Nanjing Normal University, College of Life Sciences, Jiangsu Key Laboratory for Biodiversity and Biotechnology & Jiangsu Key Laboratory for Aquatic Crustacean Diseases, Nanjing 210023, Jiangsu, China.
[2] Jiangsu Second Normal University, College of Life Science, Chemistry and Chemical Engineering, Nanjing 210023, Jiangsu, China.
[3] Co-Innovation Center for Marine Bio-Industry Technology of Jiangsu Province, Lian Yungang 222005, China.

* Corresponding Author: Tel.: +86.258 5891617
E-mail: biolipeng@163.com

Received 18 September 2017
Accepted 6 February 2018

Abstract

A *Caspase-14* gene homolog (designated as *PsCaspase-14*) in a reptile, the Chinese soft-shelled turtle *Pelodiscus sinensis* (Wiegmann, 1835), has been cloned and identified. The full-length cDNA of turtle *PsCaspase-14* was consisted of 1,464 nucleotides with a 5'-terminal untranslated region (UTR) of 45 base pairs (bp), a 3'-terminal UTR of 198 bp with a canonical polyadenylation signal sequence AATAAA, and an open-reading frames of 1,068 bp, which encoding 406 amino acids (Theoretical pI/Mw: 6.77/46.24kDa) and containing PAAD-DAPIN domain (52-133) and CASc domain (170-406). Sequence alignment, phylogenetic analyses, and structure comparison revealed that *PsCaspase-14* is a member of the Caspase family. The Chinese soft-shelled turtles were infected with *Aeromonas hydrophila* and *Vibrio parahaemolyticus*, and their innate immune responses were investigated from *PsCaspase-14* mRNA expression levels in various tissues by using real-time PCR method. RT-qPCR analyses showed that turtles *PsCaspase-14* mRNA was ubiquitously expressed in brain, liver, heart, lung, stomach, spleen, muscle, pancreas, gallbladder, kidney, and intestine tissues of control turtles, and RT-qPCR analyses further indicated that *PsCaspase-14* mRNA was affected significantly in tissues of the turtles challenged by bacteria *A. hydrophila* and *V. parahaemolyticus*, suggesting that *PsCaspase-14* might be involved in turtle antiviral immunity.

Keywords: *Pelodiscus sinensis*, *PsCaspase-14*, cDNA cloning, mRNA expression, Immune challenge.

Introduction

Caspases (cysteine-dependent aspartyl-specific protease) belong to a family of cysteine proteases that cleave target proteins at specific aspartate residues (Alnemri *et al*., 1996; Nicholson *et al*., 1995; Julien *et al*., 2016) and mediate proteolytic events indispensable for biological phenomena such as inflammation cell death or apoptosis (Sadowski-Debbing *et al*., 2002; Brynychova *et al*., 2016; Larsen & Sorensen 2017). It is now clear that caspases are thought to play a pivotal role in apoptosis as an evolutionarily conserved function (Seidelin *et al*., 2013). Up to now, numerous caspases have been identified in various animals from sponges to vertebrates (Sakamaki & Satou, 2009). Using the positions of introns as stable characters during recent vertebrate evolution, Eckhart *et al* defined 3 phylogenetic clades of caspase genes: *caspases-1, -2, -4, -5, -9, -12, -14, -15, -16* (clade I), *caspases-3, -6, -7, -17* (clade II), and *caspases-8, -10, -18, CFLAR* (clade III) (Eckhart *et al*., 2008; Man & Kanneganti 2015). In November 2017, a PubMed search of the word "caspase" reveals several thousand (> 84,200) of publications related to caspases in various functional roles (Lone *et al*., 2015; Larsen & Sorensen 2017; Lee *et al*., 2017). However the *Caspase-14* was confirmed exist in the skin to protect us against UVB radiation rather than related to apoptosis (Denecker *et al*., 2007).

The Chinese soft-shelled turtle (*Pelodiscus sinensis* (Wiegmann, 1835)), previously known as *Trionyx sinensis*, was important commercially reptile that cultured in fresh water in Southeast Asia, especially in China, Japan and Korea (Chen *et al*., 1999), for its good nutriment and medical values. Nevertheless, infectious diseases caused by bacteria and virus have caused severe losses to turtle culture industry (Chen *et al*., 1999; Hsieh *et al*., 2006; Lu & Jin, 1996; Zhao *et al*., 2007). Some studies have demonstrated that infection with *Aeromonas hydrophila* resulted in various diseases of soft-shelled turtles, such as septicemia, furunculosis, and red neck diseases (Zhou *et al*., 1999; Zhou *et al*., 2011). Previous reports showed that *Vibrio parahaemolyticus* was a curved, rod-shaped, Gram-negative, bacterium found in brackish saltwater, which was one of the most important pathogens and has caused great loss in

aquaculture (Cai *et al*., 2006; Choudhury *et al*., 2016). Turtles have to regulate expression of many of their genes to cope with varying environments and even microbial infection as part of their survival strategies (Bo *et al*., 2012; Liu *et al*., 2010; Yamashita *et al*., 2004). However, the caspases in turtles have not been characterized. It remains unknown how the caspases were expressed in turtles in response to microbial pathogens infection. This study aimed to characterize the genetic structure of the *Caspase-14* gene (named as *PsCaspase-14*) from the Chinese soft-shelled turtles and to analyze its mRNA expression patterns in different tissues under immune challenge with *A. hydrophila* and *V. parahaemolyticus*, respectively.

Materials and Methods

Animal and Sample Preparation

A. hydrophila (Collector number: 1.2017) and *V. parahaemolyticus* (Collector number: 1.1614) were purchased from China General Microbiological Culture Collection Center (CGMCC, Beijing, China). After rejuvenation, the strain was static cultured in Luria Bertani (LB) broth medium at 28°C for 24 h. Then the bacteria were collected by centrifugation (3000 g for 10 min at 4°C) and diluted into 1×10^7 colony-forming units (CFU)/mL in sterile normal saline solution (0.65% NaCl).

Ninety healthy experimental Chinese soft-shelled turtles (5-8 g in body weight) were sampled from aquaculture farm and reared in clean tanks of our laboratory for more than 30 days. Thirty (each time point of the infection with five individuals) were injected intraperitoneally with live *A. hydrophila* (1.0×10^7 CFU/5 g body weight) and introduced into clean tanks. Thirty were injected intraperitoneally with live *V. parahaemolyticus* (1.2×10^6 CFU/5 g body weight) and introduced into clean tanks. Thirty were injected with sterile normal saline (PBS) and served as control. All infected turtles began to show some clinical syndromes such as lethargy, hyperaemia, ulcers and scars in the abdomen 2 days after injection, while controls showed no clinical symptoms. All procedures adopted in this study were approved by the Institutional Animal Care and Use Committee of the Nanjing Normal University (SYXK(Jiangsu)2015--0028). The turtles infected by *A. hydrophila* and control turtles were respectively euthanized at 6 h, 24 h (1 d), 48 h (2 d), 72 h (3 d), 4 d, and 5 d after infection. Meanwhile, the turtles infected by *V. parahaemolyticus* and control turtles were respectively euthanized at 6 h, 12 h, 24 h, 36 h, 48 h, and 72 h after infection. Various tissues samples (brain, liver, heart, lung, stomach, spleen, muscle, pancreas, gallbladder, kidney, and intestine) were collected from infected and control turtles. The samples (about 5-15 mg for each sample) were isolated at the six sampling time points, respectively. Various samples were dissected and preserved in RNA*later* RNA Stabilization Reagent (Qiagen, Germany), cut into tiny particles (less than 0.2 mm thick) in separate tubes, kept overnight at 4°C, and finally stored at -20°C before total RNA isolation.

Total RNA Isolation and RT-PCR

Total RNA from various tissues was extracted separately using the RNeasy Mini Kit (Qiagen, Germany) according to the instruction manual. The quality and quantity of total RNA were determined by agarose gel electrophoresis and absorbance spectrophotometry in a BioPhotometer (Eppendorf, Germany). The cDNAs used to obtain 5'- and 3'-end sequences of each gene were synthesized using 5' RACE System for Rapid Amplification of cDNA Ends, Version 2.0 (Invitrogen, USA) and SMART™ RACE cDNA Amplification Kit (Clontech, USA) with SuperScript™ II RT (Invitrogen, USA) according to the user's manual. The synthesized cDNA was stored at -80°C until used.

Cloning the Full-Length cDNA Sequence of *PsCaspase-14*

The full-length cDNA sequence of the *PsCaspase-14* gene were made up of 5' RACE segments, expressed sequence tag (EST) segment and 3' RACE segments. Based on EST (548 bp, GenBank accession number FF281776) sequence information, new gene-specific primers (Table 1) were designed and synthesized to obtain the full-length cDNA sequence. Primers including Abridged Anchor Primer (10 μM), Anchor Primer (10 μM), AUAP or UAP (10 μM), and Caspase-G51/Caspase-G52 for *PsCaspase-14* were employed to amplify the 5'-ends of each cDNA, while 10× Universal Primer A Mix (UPM) and Caspase-G3 for *PsCaspase-14* was employed to obtain the 3'-ends of each cDNA. Finally, the *PsCaspase-14* open reading frame (ORF) was amplified using primer pair Caspase-QCF/Caspase-QCR (Table 1). The polymerase chain reaction (PCR) for 5'-RACE reactions were carried out respectively in a 50 μL reaction mixture: (1), the primary PCR containing 5 μL 10 × PCR buffer, 3 μL $MgCl_2$ (25mM), 1 μL dNTP Mix (10 mM), 2 μL Abridged Anchor Primer (10 μM), 31.5 μL sterilized water, 0.5 μL *Taq* DNA polymerase (5 units/μL), 2 μL gene-specific primer (10 μM) and 5 μL of RACE-Ready cDNA, and finally overlay with 50 to 100 μL of mineral oil. (2), the nested PCR containing 5 μL 10 × PCR buffer, 3 μL $MgCl_2$ (25 mM), 1 μL dNTP Mix (10 mM), 1 μL AUAP or UAP (10 μM), 33.5 μL sterilized water, 0.5 μL *Taq* DNA polymerase (5 units/μL), 1 μL gene-specific primer (10 μM) and 5 μL dilution of primary PCR product, and finally overlay with 50 to 100 μl of mineral oil. The PCRs for both the 3' and 5' RACE were carried out on a thermal cycler S1000™ (Bio-Rad, Hercules, CA, USA) with an initial denaturation step of 94°C for 3-5

Table 1. Primers used for for gene cloning and real-time quantitative PCR quantification. (F: forward primer and R: reverse primer).

Application	Primers Information	Primer Sequence (5′–3′)	Amplicon length (bp)
5'-RACE	Abridged Anchor Primer (AAP)	GGCCACGCGTCGACTAGTACGGGGGGGGGG	
	Abridged Universal Amplification Primer (AUAP)	GGCCACGCGTCGACTAGTAC	
	Universal Amplification Primer (UAP)	CUACUACUACUAGGCCACGCGTCGACTAGTAC CUACUACUACUAGGCCACGCGTCGACTAGTACGGGGGGGGGG	
	Anchor Primer (AP)		
	Caspase-G51	ATAAGAGTGATGAGGCAGCAGC	805 bp
	Caspase-G52	GGAGCCTGAAGTGAGAAGTATC	1023 bp
3'-RACE	10× Universal Primer A Mix (UPM)	Long: CTAATACGACTCACTATAGGGCAAGCAGTGGTATCAACGCAGAGT	
	Nested universal primer (NUP)	Short: CTAATACGACTCACTATAGGGC CCAGGATCGTTGAAGCAATGGATGAAGTC	382bp
	Caspase-G3		
ORF full-length confirmation qPCR	Caspase-QCF	CGAGATGGTTGTTTTCCGCG	1232 bp
	Caspase-QCR	CAGCCTGTTAAGGTGCAAGGTAC	
	β-actin-qF	TGGCACCACACCTTCTACAATG	178 bp
	β-actin-qR	AGGCGTACAGGGACAACACA	
	Caspase-qF	CTTCTCACTTCAGGCTCCCAAC	150 bp
	Caspase-qR	TATGCCACTCTGTGCCATCCT	

min, followed by 30-35 cycles of 94°C for 0.5-1 min, 55°C for 0.5-1 min and 72°C for 1-2 min. Extra extension at 72°C for 5-7 min, indefinite hold at 5°C until products are removed. The PCR product was separated on a 2% agarose gel, and bands with expected sizes was cut from the gel and purified using a gel purification kit (Ayxgen). The freshly purified PCR product was cloned into the pGEM®-T Easy Vectors Systems (Promega, USA), and transformed into competent *Escherichia coli* cells DH5α (TaKaRa, Dalian, China). The positive transformants were picked using a blue-white screen, and inserts were verified by PCR. Three of the positive clones were sequenced on an ABI PRISM 3730 Automated Sequencer using BigDye terminator v3.1 Cycle Sequencing Kit (Applied Biosystems, USA). The sequences obtained after 5'- and 3'-RACE were assembled using DNAStar Lasergene 7.1 software to generate full-length cDNA.

Expression Patterns of *PsCaspase-14* gene in *P. sinensis* Challenged with Bacteria

The mRNA expression patterns of *PsCaspase-14* in various tissues with respect to different immune challenge stress were examined using real-time fluorescent quantitative PCR (RT-qPCR) method.

Total RNA from various samples (n=3, each replicate was pooled from 3 turtle individuals) was isolated using RNeasy Mini Kit (Qiagen, Germany). The cDNA first-strand synthesis was carried out based on TOYOBO ReverTra Ace® qPCR RT Kit (Toyobo, Japan) and served as template. cDNA mix was diluted to 1:10 with Milli-Q water (Toyobo, Japan) and stored at −80°C for subsequent RT-qPCR. In this study, all primers used for RT-qPCR were designed respectively according to the corresponding sequences (XM_006112915.1 for *β-actin*, JQ864323.1 for *PsCaspase-14*) of *P. sinensis*. Two primer sets were designed to perform real-time PCR using TOYOBO SYBR® Green Realtime PCR Master Mix (TOYOBO, Japan) in Funglyn FTC-3000 (Funglyn Biotech Inc, Canada). *β-actin* was used as internal standard as it was proved previously to be housekeeping gene during various stimulus (Li *et al*., 2015). Negative controls missing cDNA template were included in this experiment. The total amount of cDNA was calibrated on the basis of the amplification of turtle *β-actin*. The cDNA was properly diluted and used as a template in PCR reactions. The cDNA was subjected to RT-qPCR amplification using two pairs of specific primers (β-actin-qF/β-actin-qR and Caspase-qF/Caspase-qR, see Table 1). The real-time PCR was carried out using 2 μL of cDNA as a template in a 20 μL reaction mixture with a denaturation step of 95°C for 30 s, followed by 40 cycles consisting of 95°C for 5 s, 60°C for 30 s,, and a finally dissociation 95°C for 15 s, 60°C for 30 s, 95°C for 15 s. The PCR products were electrophoresed on a 1.0% agarose gel stained with ethidium bromide. The relative magnitudes of expression (fold change) of the tested gene were calculated using the $2^{-\Delta\Delta Ct}$ method (Livak & Schmittgen, 2001). The tests were carried out in triplicate and all data are represented as mean ± standard error (SE), and the statistical procedures were conducted using SPSS Statistics 20.0 (SPSS Inc., Chicago, IL, USA). Date was determined by one-way analysis of variance (ANOVA) and Turkey's

post-hoc Duncan's multiple range tests. P<0.05 was considered to be significantly different.

Sequences Analyses of *PsCaspase-14* gene

PsCaspase-14 cDNA sequence was analyzed based on nucleotide and protein databases using the BLASTX and BLASTN program. The open reading frame (ORF) of *PsCaspase-14* cDNA was determined using ORF Finder. Molecular mass and theoretical isoelectric point was predicted using Compute pI/Mw tool. The potential N-linked glycosylation sites were predicted on NetNGlyc 1.0 Server according to the Asn-X-Ser/Thr rule. The *PsCaspase-14* amino acid sequence, plus others Caspase amino acid sequences retrieved from the National Center for Biotechnology Information (NCBI) protein database, was subjected to ClustalW2 for multiple sequence alignment. Motif scan was respectively performed against databases of motifs and by Simple Modular Architecture Research Tool (SMART). The putative signal peptide was predicted using SignalP 4.0. The potential protein subcellular localization was predicted on the PRORT II. Three-dimensional domain structure of PsCaspase was predicted by SWISS-MODEL Server. Additional assessments of domain structures were performed on ProSA-Web and Verify3D Structure Evaluation Server. Transmembrane topology prediction was performed using TMHMM Server v. 2.0 and DAS-TMfilter Server.

Results

Identification and Characterization of Soft-Shelled Turtle *PsCaspase-14* gene

Several fragments (805 bp and 1,023 bp) were amplified by 5′-RACE technique from the 5′ end of each cDNA, respectively. One fragment (382 bp) was amplified by 3′-RACE technique. The ORF was further amplified with specific primers and produced a 1,232 bp fragment for *PsCaspase-14*.

The above sequence data indicated a 1,464 bp full-length *PsCaspase-14* cDNA with a 1,221 bp ORF starting at nucleotide 46 and stopping at nucleotide 1266, which encodes 406 amino acid residues with a putative molecular mass of 46.24 kDa and a calculated theoretical isoelectric point of 6.77. The *PsCaspase-14* cDNA included a 45 bp 5′-terminal untranslated region (UTR) and a 198 bp 3′-terminal UTR. Additionally, stop codon TAA, canonical polyadenylation signal (AATAAA located at nucleotide 1423-1428) and poly-(A) tail were found in the 3′ end of the *PsCaspase-14* cDNA (Supplementary Figure S1). The deduced amino acid

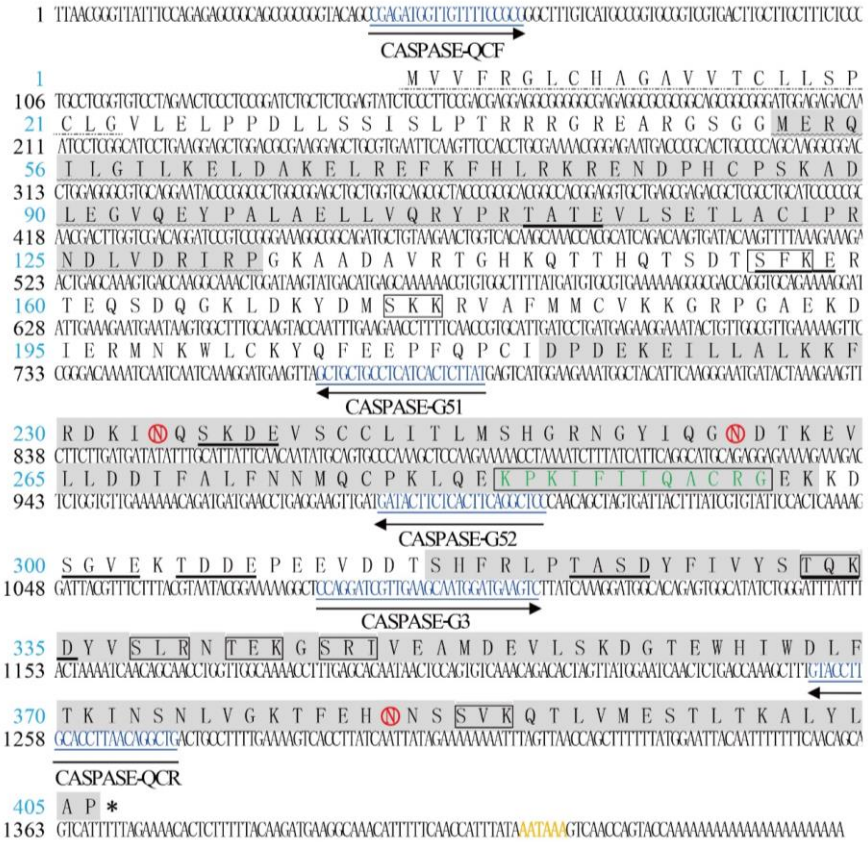

Supplementary Figure S1. Structures of full-length cDNA sequences and deduced amino acid sequences of *PsCaspase-14* in *Pelodiscus sinensis*. The putative polyadenylation signals (AATAAA) were marked in yellow and bold. The stop codons were indicated by asterisk (*). Sequences of the primers used for obtaining open reading frame fragments (CASPASE-QCF and CASPASE-QCR for *PsCaspase-14*) and RACE products (CASPASE-G51/CASPASE-G52 and CASPASE-G3 for *PsCaspase-14*) were underlined and marked in blue from the 5'- to 3'-end. Three Caspase family signatures sequences in *PsCaspase-14* were showed respectively. Deduced Caspase family cysteine active site was boxed in shaded region and highlighted as marked in green. Three N-glycosylation sites were circled in red. Signal peptides sequence of *PsCaspase-14* was underlined by dotted line. Protein kinase C phosphorylation sites were double underlined.

sequences of PsCaspase-14 revealed several canonical features of the Caspase family. Which containing PAAD_DAPIN domain (52-133) and CASc domain (170-406), and there was a deduced caspase cysteine active site in the CASc domain, KPKIFIIQACRG (aa 284–295). The C+G content in the *PsCaspase-14* was 45.3%. The nucleotide and amino acid sequences of the *PsCaspase-14* closely match those of *Caspase-14* in other species and the identity scores range from 74% to 98% at nucleotide levels, and 45% to 99% at amino acid levels. The 1,464 bp nucleotide sequence representing the full-length cDNA sequence of the *PsCaspase-14* gene which was obtained by cluster analysis of the RACE-PCR amplification fragments and the EST sequence. The *PsCaspase-14* cDNA sequence was assigned GenBank accession numbers JQ864323.1.

Phylogenetic Analysis Using Caspase-14 Sequences

The phylogenetic analyses of the Caspases-14 amino acid dataset generated Maximum-Likelihood tree topologies (Supplementary Figure S2). The ML tree revealed two major subgroups of Caspase molecules, one branch marked in pink was composed of mammals, and the others marked in purple included the reptiles together with the turtle in this study, in which there were two different Caspases-14 of the Chinese soft-shelled turtle, one of which was downloaded from NCBI (XP_006121825.1), another was got from RACE-PCR amplification in this study. The ML tree showed the Caspase-14 of the Chinese soft-shelled turtle and Chelonia falling into the same sublineage. The results suggested that the sequence of *PsCaspase-14* gene was correct and solid.

Structural Analyses of *PsCaspase-14*

Protein motif domains scanning from SMART database diagram indicated PsCaspase-14 protein contains PYRIN domain (from 52 to 133 amino acid residues) and CASc domain (from 170 to 406 amino acid residues). The potential protein subcellular localization prediction indicated that PsCaspase-14 protein was likely to locate in extracellular (55.6%), nucleus (22.2%), vacuolar (11.1%), mitochondrial (11.1%). The result from SignalP revealed that PsCaspase-14 protein has a putative signal peptide found (1 to 23) and it was probably a non-secretory protein. Transmembrane topology prediction indicated that PsCaspase-14 protein was probably a transmembrane protein (transmembrane helices length between 15 and 33). PsCaspase-14 protein posed a QACRG motif, with an absolute requirement for the active site cysteine, and the C and G were conserved in known Caspases (Wang *et al*., 2008). The three-dimensional structure analysis of PsCaspase-14 protein revealed that it contains eleven α helices and ten twisted β-sheets. Nests such as LYS 284, PRO 285, LYS 286, ILE 287, PHE 288, ILE 289, ILE 290

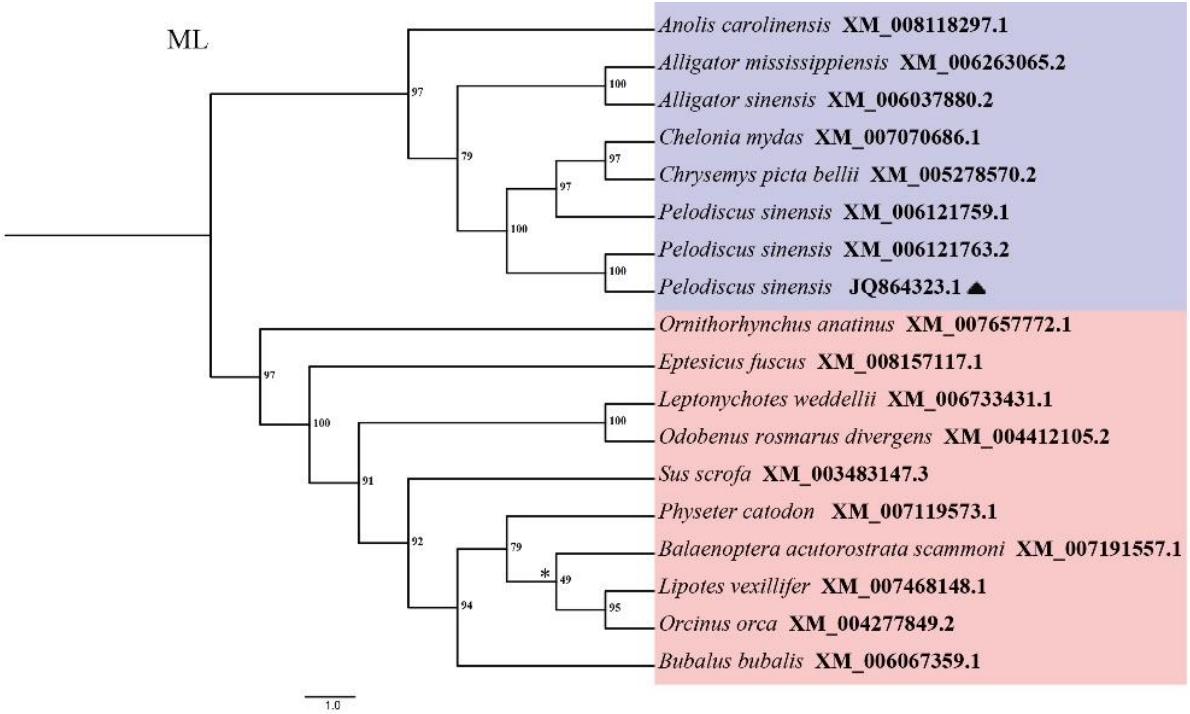

Supplementary Figure S2. Phylogenetic analysis of PsCaspase-14 protein and other representative Caspase-14 protein were inferred using the Maximum-Likelihood. Bootstrap values greater than 50% for Maximum-Likelihood (ML) analysis was shown above major branches. The scale bar represents 1.0 substitutions per site. An asterisk indicates a branch having less than 50% bootstrap values support.

GLN 291, ALA 292, CYS 293, ARG 294 and GLY 295, were located in this β-sheets and loop chains, which form cysteine active site.

Tissue Distribution of *PsCaspase-14* in *P. sinensis* after Bacteria (*A. hydrophila* and *V. parahaemolyticus*) Challenge

The expression levels of *PsCaspase-14* mRNA in the brain, liver, heart, lung, stomach, spleen, muscle, pancreas, gallbladder, kidney, and intestine of the Chinese soft-shelled turtle were examined by real-time fluorescent quantitative PCR. The relative gene expression levels were calculated by $2^{-\Delta\Delta Ct}$ method, with the expression levels of *PsCaspase-14* mRNA in PBS control used as a calibrator, respectively. The mRNA expression levels of *PsCaspase-14* in different tissue were indicated as n-fold differences relative to the calibrator (Figures 1 to 4). The RT-qPCR result showed that the *PsCaspase-14* was mainly expressed in most detected tissues after infected with *A. hydrophila* and *V. parahaemolyticus* except muscle testing at 6 h, lung testing at 48 h and spleen testing at 4 d after *A. hydrophila* infection, and the expression levels among the tissues were various at 6 h, 24 h, 48 h, 72 h, 4 d, 5 d and 6 h, 12 h, 24 h, 36 h, 48 h, 72 h respectively (Figures 1 to 4). Statistical significance was indicated with an asterisk (* mean $p < 0.05$ and ** mean $p < 0.01$) between tissues injection with bacteria (*A. hydrophila* or *V. parahaemolyticus*) and tissues injection with PBS. Different lowercase letters indicating statistical significantly among different time points post-injection with bacteria (Tukey's *post hoc* test, $\alpha = 0.05$). The *PsCaspase-14* mRNA expression of multifarious tissues after exposure to the *A. hydrophila* infection was fluctuated at detected time points (Figures 1, 2), while the expression was obviously different over time in all the detected tissues after the *V. parahaemolyticus* infection compared with the controls (Figures 3, 4).

Expression Patterns of *PsCaspase-14* in Response to Immune Challenge Stress (*A. hydrophila* and *V. parahaemolyticus*)

As shown in Figure 1, the *PsCaspase-14* mRNA was expressed in all detected tissues under live PBS and *A. hydrophila* challenge at intervals (6 h, 24 h, 48 h, 72 h, 4 d, 5 d), while the results in Figure 3 reflected the difference between the experimental group and control group more clearly, while also presenting a trend of mRNA expression in various

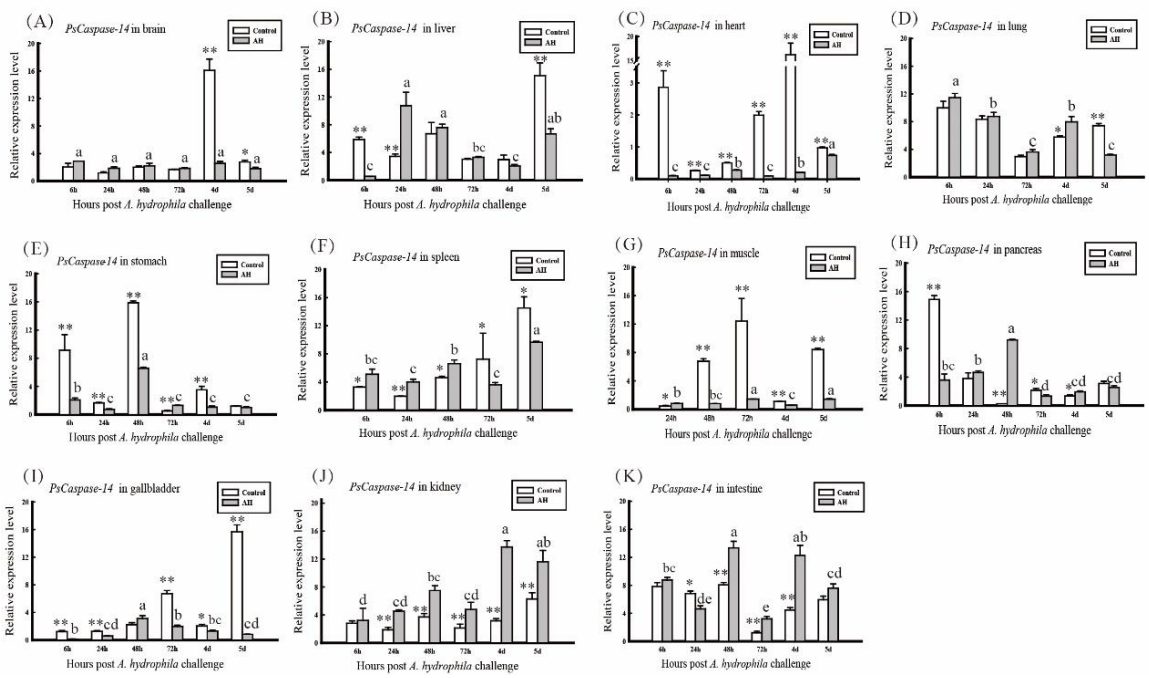

Figure 1. Tissue for time-*PsCaspase-14* infected by *A. hydrophila*.
PsCaspase-14 mRNA expression in brain (A), liver (B), heart (C), lung (D), stomach (E), spleen (F) muscle (G), pancreas (H), gallbladder (I) kidney (J), and intestine (K) tissues of *Pelodiscus sinensis* in response to *Aeromonas hydrophila* challenge (black bars) at 6 h, 24 h, 48 h, 72 h 4 d and 5 d. Tissues collected from turtles injected with *A. hydrophila* (gray bars) and PBS (white bars) were compared with respect to *PsCaspase-14* mRNA expression (relative to *β-actin*) using Tukey's *post hoc* test. Bars represent mean ± S.E. of three independent investigations. Statistical significance was indicated with an asterisk between tissues injection with *A. hydrophila* and PBS. *$p < 0.05$ and **$p < 0.01$. Different lowercase letters indicating statistical significantly among different time points post-injection with *A. hydrophila* (Tukey's *post hoc* test, $\alpha = 0.05$). *h*, hours post-challenge. Unfortunately, the *PsCaspase-14* mRNA expression in lung testing at 48 h (Figure 1-D), spleen testing at 4 d (Figure 1-F) and muscle testing at 6 h (Figure 1-G) were undetected, so the three fluorescence quantitative results were not shown in the Figure 1.

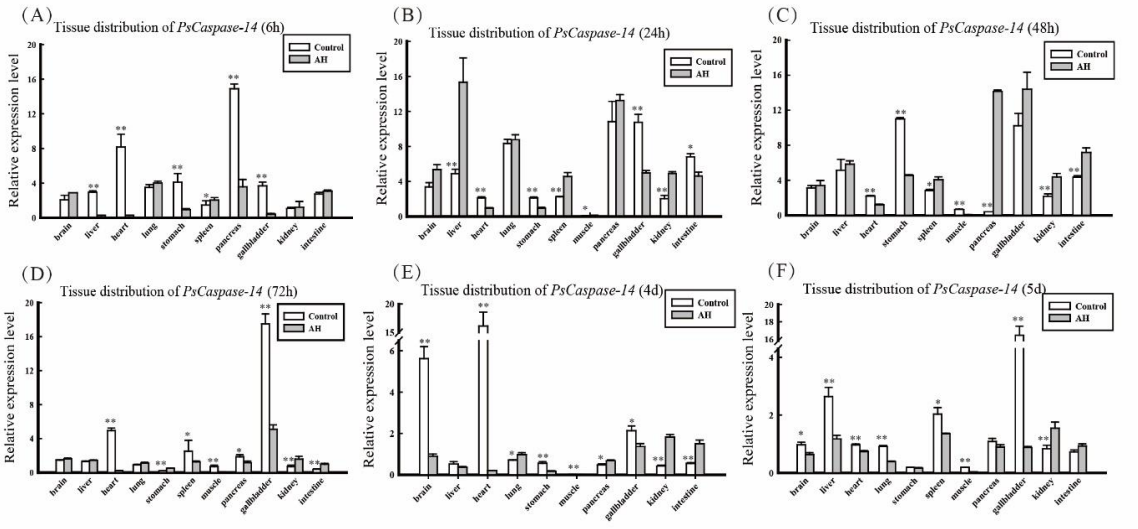

Figure 2. Time for tissue-*PsCaspase-14* infected by *A. hydrophila*.
Tissue distribution of *PsCaspase-14* mRNA in brain, liver, heart, lung, stomach, spleen, muscle, pancreas, gallbladder, kidney, and intestine tissues of *Pelodiscus sinensis* at different time periods after *Aeromonas hydrophila* infection. Fold expression relative to *β-actin* was calculated as $2^{-\Delta\Delta Ct}$. *h*, hours post-challenge. Statistical significance is indicated with an asterisk between tissues injection with *A. hydrophila* and PBS. $*p < 0.05$ and $**p < 0.01$. Unfortunately, the *PsCaspase-14* mRNA expression in muscle testing at 6 h (Figure 2-A), spleen testing at 4 d (Figure 2-E) and lung testing at 48 h (Figure 2-C) were undetected, so the three fluorescence quantitative results were not shown in the Figure 2.

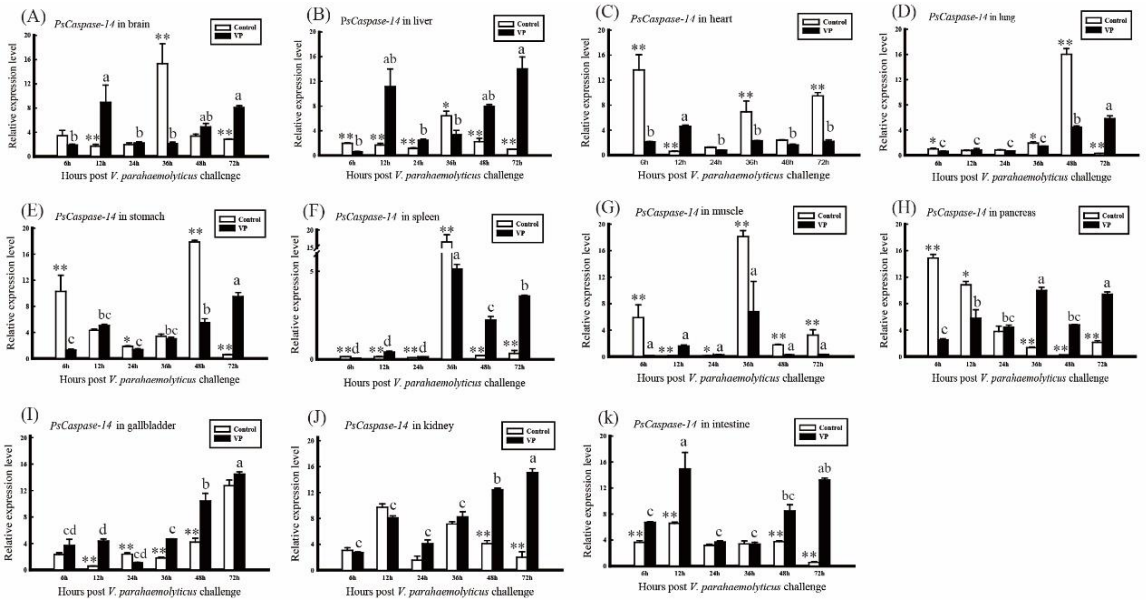

Figure 3. Tissue for time-*PsCaspase-14* infected by *V. parahaemolyticus*.
PsCaspase-14 mRNA expression in brain (A), liver (B), heart (C), lung (D), stomach (E), spleen (F) muscle (G), pancreas (H), gallbladder (I) kidney (J), and intestine (K) tissues of *Pelodiscus sinensis* in response to *Vibrio parahaemolyticus* challenge (black bars) at 6 h, 12 h, 24 h, 36 h, 48 h and 72 h. Tissues collected from turtles injected with *V. parahaemolyticus* (black bars) and PBS (white bars) were compared with respect to *EsHSC70-3* mRNA expression (relative to *β-actin*) using Tukey's *post hoc* test. Error bars represent mean ± S.E. of three independent investigations. Statistical significance was indicated with an asterisk between tissues injection with *V. parahaemolyticus* and PBS. $*p < 0.05$ and $**p < 0.01$. Different lowercase letters indicating statistical significantly among different time points post-injection with *V. parahaemolyticus* (Tukey's *post hoc* test, $\alpha = 0.05$). *h*, hours post-challenge.

organizations over time. The mRNA expression of *PsCaspase-14* in the tissue of brain peaked at 4 d in the PBS group, but it was almost stable in the experimental group after the *A. hydrophila* infection (Figure 1-A). In the tissues of the liver, heart, stomach, pancreas and gallbladder, we can obviously be informed that the *PsCaspase-14* expression was significantly reduced at the beginning when the tissues were infected by *A. hydrophila* (Figures 1-B, 1-C, 1-E, 1-H, 1-I). The expression levels soared

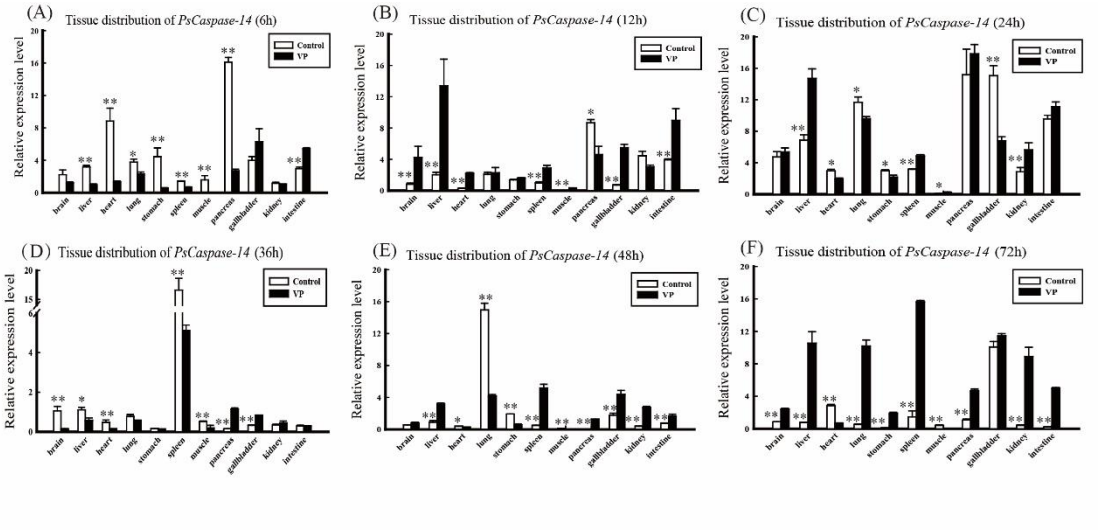

Figure 4. Time for tissue -*PsCaspase-14* infected by *V. parahaemolyticus*.
Tissue distribution of *PsCaspase-14* mRNA in brain, liver, heart, lung, stomach, spleen, muscle, pancreas, gallbladder, kidney, and intestine tissues of *Pelodiscus sinensis* at different time periods after *Vibrio parahaemolyticus* infection. Fold expression relative to *β-actin* was calculated as $2^{-\Delta\Delta Ct}$. *h*, hours post-challenge. Statistical significance was indicated with an asterisk between tissues injection with *V. parahaemolyticus* and PBS. **p* < 0.05 and ***p* < 0.01.

significantly after 24 hours of testing in the liver (Figure 1-B), and this result shows that infected external bacteria indicated the liver may had made a stress response. The mRNA expression of *PsCaspase-14* was down-regulated in an interval time (48 h to 4 d), and no significant difference was detected between the control group and the experimental group. Nevertheless, the expression levels of *PsCaspase-14* was soared significantly at 5 d, while this phenomenon was not observed in experimental group after infected by *A. hydrophila* (Figure 1-B). After 6 hours of *A. hydrophila* infection, the expression levels of the *PsCaspase-14* mRNA in the heart tissue of the experimental group was significantly lower than that of PBS control group (Figure 1-C). The *PsCaspase14* had a constant expression in the lungs on the first four days after they were injected by *A. hydrophila*. However, the expression levels began to regulate downwards at 5 d, which indicated the appearance of a late immune stress response (Figure 1-D). Although the mRNA expression of *Pscaspase-14* in the stomach and pancreas were initially affected by the injection of *A. hydrophila*, this kind of influence was weak, and returned to normal after 5 d (Figures 1-E, 1-H). Compared with the PBS control group (after 6 h to 48 h), the *PsCaspase-14* mRNA expression in the spleen gradually increased after the infection of *A. hydrophila* (Figure 1-F). In the muscle, the mRNA expression of *PsCaspase-14* showed increasing at 6 h after the *A. hydrophila* injection, but it dropped significantly more than the PBS control group after 48 h post-challenge (Figure 1-G). The *PsCaspase-14* dropped significantly in the gallbladder after *A. hydrophila* infection, and went through a process of up-regulated at 48 h and ended up significant lower than that of the PBS control group in the following detected point in time (Figure 1-I). The *PsCaspase-14* mRNA expression in the kidney increased significantly after the *A. hydrophila* injection ($P < 0.01$) at 48 h (Figure 1-J). The *PsCaspase-14* mRNA expression at 6 h in the intestine showed no significant difference between the experimental and control group (Figure 1-K), despite being significantly lower than that of PBS control group at 24 h after the *A. hydrophila* infection. The mRNA expression level of the *PsCaspase-14* was up-regulated and significantly higher than that of the control group until 4 d ($P < 0.01$), while the expression difference was not significant at 5 d.

In response to *V. parahaemolyticus* challenge, the expression levels of *PsCaspase-14* mRNA were increased at 12 h compared with 6 h and higher than that of the PBS control group in the brain, liver, heart, lung, stomach, and muscle tissue after injection. Nevertheless, the *PsCaspase-14* mRNA expression in various tissues was widely different from their corresponding PBS control group and changed arbitrarily over time after 24 hours injection of *V. parahaemolyticus* (Figures 3-A, 3-B, 3-C, 3-D, 3-E, 3-G). Compared with PBS control group, the expression levels of *PsCaspase-14* in the tissues of heart and muscle were significantly lower ($P < 0.01$) at 6 h (Figures 3-C, 3-G). Although the changing trends of *PsCaspase-14* mRNA expression in brain, liver, stomach, gallbladder, kidney and intestine of the PBS control group were different, the expression of experimental group induced up-regulated at first, down-regulated at 24 h and continuously rising after 36 h (Figures 3-A, 3-B, 3-E, 3-I, 3-J, 3-K). These results showed that when the multicellular organism was exposed to bacterial infections, a few organizations will have similar immune response. It

also indicated that the expression of the *PsCaspase-14* was induced by bacterium (*V. parahaemolyticus*). The *PsCaspase-14* mRNA expression in the heart was down-regulated significantly in the beginning and up-regulated after 12 h, then down-regulated at 24 h and rebound slightly and tended to be stable after 48 h of the *V. parahaemolyticus* infection (Figure 3-C). The *PsCaspase-14* mRNA expression of the lung had a steadily rising trend in response to the *V. parahaemolyticus* injection, but sharp fluctuations has appeared in the PBS control group after 36 h (Figure 3-D). The *PsCaspase-14* mRNA in the spleen and pancreas infected by *V. parahaemolyticus* had similar expression trends (Figures 3-F, 3-H), and the change trends of the *PsCaspase-14* mRNA expression in spleen was similar after infection with *V. parahaemolyticus* or PBS respectively (Figure 3-F). The expression level of the *PsCaspase-14* mRNA in the muscle was relatively lower and down-regulated at 6 h after the *V. parahaemolyticus* injection, then it was up-regulated at 12 h and was higher than that of the PBS control group (Figure 3-G). The highest expression level of the *PsCaspase-14* mRNA was detected in the muscle at 36 h. After injection with *V. parahaemolyticus*, the *PsCaspase-14* mRNA expression in the gallbladder and the intestine tissues was up-regulated at the intervals (6 h, 12 h, 36 h, 42h, 72h) and the other intervals (6 h, 12 h, 24 h, 42 h, 72 h) (Figures 3-I, 3-K).

Discussions

Previous studies have confirmed that *Caspase-14* play an essential roles in maintaining the skin structure and balance of moisture, and it also function as molecular chaperones to be involved in ontogenesis, skin physiology and terminal differentiation of keratinocytes (Craen *et al*., 1998; George *et al*., 2015; Mikolajczyk *et al*., 2004). In addition, Caspase-14, a protease important for filaggrin processing, was helpful to resist atopic dermatitis (Marsella *et al*., 2016). So far there is no *Caspase-14* gene from the Chinese soft-shelled turtle cloned and characterized, and its function within the innate immune system has not been studied in detail. In this study, the results suggested that the *PsCaspase-14* may play an important role in immune response of *P. sinensis*. It was first identified from *P. sinensis* by RACE-PCR amplification and the ORF of the *PsCaspase-14* was 1,221 bp encoding a polypeptide of 406 amino acids. The Blastn search in NCBI indicated the deduced amino acid sequence of the *PsCaspase-14* share high levels of similarity to *Caspase-14* from other known organisms, especially with the *Caspase-14* (XM_006121763.2) from the Chinese soft-shelled turtle *P. sinensis* with 98% similarity and reached to 81% similarity with the one of turtles *Chrysemys picta bellii* and *Chelonia mydas*. The same results got via Blastx. Bioinformatics analyses indicated that the *PsCaspase-14* has three N-glycosylation sites, seven protein kinase C phosphorylation sites and eight Casein kinase 2 phosphorylation sites (Supplementary Figure S1). Protein domains, families and functional sites analyses showed that PsCaspase-14 protein have typical p20, p10 subunits and CYS (caspase family cysteine active site), which was consistent with the previous study that the mammalian Caspase-14 had the structure of p20 and p10 (Chowdhury *et al*., 2008), and those functional sites may play an important role in immune response (Mikolajczyk *et al*., 2004). The function of Caspase-14 was closely similar to the Caspase-1, which without death domain (DD) was a Non-apoptotic protein (Denecker *et al*., 2007; Denecker *et al*., 2008), and Caspase-1 also processes IL-1β, IL-18 and IL-33, which was responsible for both the inflammatory and the innate immune responses (Nadiri *et al*., 2006). Caspase 14 cannot be classified as either an apoptotic or inflammatory caspase and has a specialized role in the differentiation of keratinocytes 17, 18 (Man & Kanneganti, 2015). Therefore, the similar structure among PsCaspase-14 and other caspases indicated that it might be mainly involved in the innate immune response. The potential protein subcellular localization prediction indicated that the PsCaspase-14 protein was likely located in extracellular, guessing it may be conducive for organism to reply various bacterial compounds. The ML trees reconstructed based on amino acids sequences of Caspase-14 protein from different animals suggested that the PsCaspase-14 protein in *P. sinensis* was clustered to that of *Phylum chordata* (Supplementary Figure S2). Multiple sequence alignments of Caspase-14 protein sequences also revealed they were highly conserved among different animals Caspase-14 protein. The conservative characteristics and high similarity with known Caspase-14 of other known species informed us that PsCaspase-14 belonged to a family of highly conserved aspartate-specific cysteine proteases and was a member of the interleukin-1β-converting enzyme family (Chowdhury *et al*., 2008; Thornberry *et al*., 1992). Meanwhile, one interleukin-1β converting enzyme (ICE) homologue was located between deduced amino acid positions 170-406 in the PsCaspase-14 protein, in which containing QACRG (291–295) (Supplementary Figure S1), and the same structure also appeared in caspase-1 protein. Previous studies have shown that Caspase-1 drives novel protective responses in critical illness models of Salmonella infection, burn, or shock (Alvarez *et al*., 2016). The QACRG represent the core of p45 (45 kDa) precursor of caspases, which can be processed to produce the active p20 (20 kDa) and p10 (10 kDa) subunits (Barrett & Rawlings, 2001; Man & Kanneganti, 2015). These results suggested that the PsCaspase-14 protein in the Chinese soft-shelled turtle may have similar immune related physiological and biochemical functions with Caspase-1.

The RT-qPCR results demonstrated that the

PsCaspase-14 mRNA possessed broad expression spectrum in all detected eleven organs, and that was influenced significantly by injecting with bacteria *A. hydrophila* and *V. parahaemolyticus*. Previous study has reported that *A. hydrophila* and *V. parahaemolyticus* were common bacterial infections, if aquatic economic species infected can cause harm to them and make a huge economic losses to aquaculture sector (Choudhury *et al*., 2016; Am *et al*., 2016). In addition, the hepatopancreas, hemocytes, intestine, and gill etc of crustacean are immune associated tissues, and hepatopancreas and hemocytes are regarded as the most important tissues involved in immunity (Jiravanichpaisal *et al*., 2006). In this study, eleven organizations (brain, liver, heart, lung, stomach, spleen, muscle, pancreas, gallbladder, kidney, and intestine) from the Chinese soft-shelled turtle were used in experiments. The innate immune system was the first line of defense (Guan & Mariuzza, 2007). After injected with PBS or bacteria, PBS group was used as a calibrator, and the different expression profiles of *PsCaspase-14* mRNA between PBS group and experimental group were detected. The results indicated that the organisms infected with bacteria showed corresponding emergency response to adapt to current situation. Furthermore, the *PsCaspase-14* expression levels in different organs were affected by injection of bacteria. In this study, after the injection of different bacteria *A. hydrophila* and *V. parahaemolyticus*, the levels of *PsCaspase-14* mRNA expression in same tissues of *P. sinensis* were also varied. Therefore, multicellular organisms would make a different response to cope with the external environment when faced with different bacteria environment. In addition to the existence of virulence factors in the organism, the host immune response to infection influenced the severity of infection (Galindo *et al*., 2006). In 2015, the aspects of caspase family of cysteine proteases in innate immunity was highlighted (Man & Kanneganti, 2015). But so far little is known about *Caspase-14* gene on the immune function and the molecular mechanism of anti-bacteria immune response in reptiles. In this study, the *PsCaspase-14* gene differentially expressed in the Chinese soft-shelled turtle experimentally infected with *A. hydrophila* or *V. parahaemolyticus* illustrated that the *PsCaspase-14* gene might be involved in antiviral immunity of *P. sinensis.*

In summary, we have identified and characterized the *PsCaspase-14* gene from the Chinese soft-shelled turtle. The *PsCaspase-14* was ubiquitous expressed in the eleven tissues tested in this study. The *PsCaspase-14* transcripts exhibited diverse levels of induction by *A. hydrophila* and *V. parahaemolyticus* challenge. Meanwhile, different expression levels of the *PsCaspase-14* were found among different tissues during infected with *A. hydrophila* or *V. parahaemolyticus*. According to the results of molecular characterization and expression patterns, it could be deduced that the *PsCaspase-14* might be involved in anti-bacterial immune responses and presented different immune responses to different bacteria. Further studies will be necessary to identify additional caspase family members of turtles and to clarify their innate immune responses to different environmental and physiological stresses.

Electronic Supplementary Material

The online version of this article contains supplementary material, which is available to authorized users.

Acknowledgements

This work was supported by grants from Innovative Team Project of Nanjing Normal University (0319PM0902), the Natural Science Foundation of the Jiangsu Higher Education Institutions of China (Grant No. 12KJB180005 to YFQ and Grant No. 17KJD240001 to PL), Priority Academic Program Development of Jiangsu Higher Education Institutions to PL and JY, and Top-notch Academic Programs Project of Jiangsu Higher Education Institutions (TAPP).

References

Alnemri, E.S., Livingston, D.J., Nicholson, D.W., Salvesen, G., Thornberry, N.A., Wong, W.W., & Yuan, J. (1996). Human ICE/CED-3 protease nomenclature. Cell 87, 171. http://dx.doi.org/10.1016/S0092-8674(00)81334-3.

Alvarez, D. F., Housley, N., Koloteva, A., Zhou, C., O'Donnell, K., & Audia, J. P. (2016). Caspase-1 activation protects lung endothelial barrier function during infection-induced stress. American Journal of Respiratory Cell & Molecular Biology, 55(4), 500. http://dx.doi.org/10.1165/rcmb.2015-0386OC.

Am, A., Silvester, R., Alexander, D., M N, & Abdulla, M. H. (2016). Characterization of blooming algae and bloom-associated changes in the water quality parameters of traditional pokkali cum prawn fields along the south west coast of india. Environmental Monitoring & Assessment,188(3). http://dx.doi.org/10.1007/s10661-016-5133-6.

Barrett, A.J., & Rawlings, N.D. (2001). Evolutionary lines of cysteine peptidases. Biological Chemistry 382, 727. http://dx.doi.org/10.1515/BC.2001.088.

Bo, J., Giesy, J.P., Ye, R., Wang, K.J., Lee, J.S., & Au, D.W. (2012). Identification of differentially expressed genes and quantitative expression of complement genes in the liver of marine medaka *Oryzias melastigma* challenged with *Vibrio parahaemolyticus*. Comparative biochemistry and physiology. Part D, Genomics & proteomics 7, 191-200. http://dx.doi.org/10.1016/j.cbd.2012.02.005.

Brynychova, V., Hlavac, V., Ehrlichova, M., Vaclavikova, R., Nemcova-Furstova, V., & Pecha, V. (2016). Transcript expression and genetic variability analysis of caspases in breast carcinomas suggests casp9 as the most interesting target. Clinical Chemistry & Laboratory Medicine, 55(1). http://dx.doi.org/10.1515/cclm-2016-0271.

Cai, L., Ji, K.F. & Hyde, K.D. (2006). Variation between freshwater and terrestrial fungal communities on decaying bamboo culms. Antonie Van Leeuwenhoek 89, 293-301. http://dx.doi.org/10.1007/s10482-005-9030-1.

Chen, Z.X., Zheng, J.C., & Jiang, Y.L. (1999). A new iridovirus isolated from soft-shelled turtle. Virus research 63, 147-151. http://dx.doi.org/10.1016/S0168-1702(99)00069-6.

Choudhury, T. G., Nagaraju, V. T., Gita, S., Paria, A., & Parhi, J. (2016). Advances in bacteriophage research for bacterial disease control in aquaculture. Reviews in Fisheries Science & Aquaculture, 25(2), 1-13. http://dx.doi.org/10.1080/23308249.2016.1241977.

Chowdhury, I., Tharakan, B., & Bhat, G.K. (2008). Caspases - an update. Comparative biochemistry & physiology Part B, Biochemistry & molecular biology 151, 10-27. http://dx.doi.org/10.1016/j.cbpb.2008.05.010.

Denecker, G., Hoste, E., Gilbert, B., Hochepied, T., Ovaere, P., Lippens, S., ... Declercq, W. (2007). Caspase-14 protects against epidermal UVB photodamage and water loss. Nature cell biology 9, 666-674. http://dx.doi.org/10.1038/ncb1597.

Denecker, G., Ovaere, P., Vandenabeele, P., & Declercq, W. (2008). Caspase-14 reveals its secrets. Journal of cell biology, 180, 451-458. http://dx.doi.org/10.1083/jcb.200709098.

Eckhart, L., Ballaun, C., Hermann, M., VandeBerg, J.L., Sipos, W., Uthman, A., ... Tschachler, E. (2008). Identification of novel mammalian caspases reveals an important role of gene loss in shaping the human caspase repertoire. Molecular biology and evolution 25, 831-841. http://dx.doi.org/10.1093/molbev/msn012.

Galindo, C.L., Sha, J., Fadl, A.A., Pillai, L.L., & Chopra, A.K. (2006). Host immune responses to *Aeromonas virulence* factors. Current Immunology Reviews 2, 13-26. http://dx.doi.org/10.2174/157339506775471910.

George, V.C., Kumar, D.R., Suresh, P.K., & Kumar, R.A. (2015). Luteolin induces caspase-14-mediated terminal differentiation in human epidermal keratinocytes. In vitro cellular & developmental biology. Animal 51, 1072-1076. http://dx.doi.org/10.1007/s11626-015-9936-5.

Guan, R., & Mariuzza, R.A. (2007). Peptidoglycan recognition proteins of the innate immune system. Trends in microbiology 15, 127-134. http://dx.doi.org/10.1016/j.tim.2007.01.006.

Hsieh, C.Y., Chang, T.C., Shen, Y.L., Chang, C.D., Tu, C., Tung, M.C., ... Tsai, S.S. (2006). Pathological and PCR detection of mycobacteriosis in pond-cultured Chinese soft shell turtles, *Trionyx sinensis*. Aquaculture 261, 10-16. http://dx.doi.org/10.1016/j.aquaculture.2006.07.005.

Jiravanichpaisal, P., Lee, B.L., & Söderhäll, K. (2006). Cell-mediated immunity in arthropods: hematopoiesis, coagulation, melanization and opsonization. Immunobiology 211, 213-36. http://dx.doi.org/10.1016/j.imbio.2005.10.015.

Julien, O., Zhuang, M., Wiita, A. P., O'Donoghue, A. J., Knudsen, G. M., & Craik, C. S. (2016). Quantitative ms-based enzymology of caspases reveals distinct protein substrate specificities, hierarchies, and cellular roles. Proceedings of the National Academy of Sciences of the United States of America, 113(14), E2001. http://dx.doi.org/10.1073/pnas.1524900113.

Larsen, B. D., & Sorensen, C. S. (2017). The Caspase-Activated DNase: Apoptosis and Beyond. FEBS Journal, 284(8), 1160-1170. http://dx.doi.org/10.1111/febs.13970.

Lee, H. J., Lee, E., Seo, Y. E., Shin, Y. H., Kim, H. S., Chun, Y. H., ... Kim, J. T. (2017). Roles of Bcl-2 and caspase-9 and -3 in CD30-induced human eosinophil apoptosis. Journal of Microbiology Immunology and Infection, 50(2), 145-152. http://dx.doi.org/10.1016/j.jmii.2015.05.017.

Li, P., Jiang, X., Sun, B., Lin, Y., Yan, J., & Zhou, K. (2015). Identification of an Alpha-Tubulin Gene from the Chinese Mitten Crab *Eriocheir sinensis*: Expression Profiles under Immune Challenge and during Larval Development. Journal Biotechnol Biomater 5, 201. http://dx.doi.org/10.4172/2155-952X.1000201.

Liu, H.W., Li.B., Liu, H., Tong, X.L., & Liu, Qin. (2010). The algorithm of high order finite difference pre-stack reverse time migration and GPU implementation. Chinese Journal of Geophysics 53, 600-610. http://dx.doi.org/10.1002/cjg2.1530.

Livak, K.J., & Schmittgen, T.D. (2001). Analysis of relative gene expression data using real-time quantitative PCR and the $2^{-\Delta\Delta CT}$ method. methods 25, 402-408. http://dx.doi.org/10.1006/meth.2001.1262.

Lone, A.G., Atci, E., Renslow, R., Beyenal, H., Noh, S., Fransson, B., ... Call, D.R. (2015). Colonization of epidermal tissue by *Staphylococcus aureus* produces localized hypoxia and stimulates secretion of antioxidant and caspase-14 proteins. Infection and immunity 83, 3026-3034. http://dx.doi.org/10.1128/IAI.00175-15.

Lu, H., & Jin, L. (1996). Studies on the *Aeromonas hydrophila* septicemia of soft-shelled turtles (*Trionyx sinensis*). Journal of Fisheries of China 203, 223-234.

Man, S. M., & Kanneganti, T. D. (2015). Converging roles of caspases in inflammasome activation, cell death and innate immunity. Nature Reviews Immunology, 16(1), 7. http://dx.doi.org/10.1038/nri.2015.7.

Marsella, R., Papastavros, V., Ahrens, K., & Santoro, D. (2016). Decreased expression of *caspase-14* in an experimental model of canine atopic dermatitis. Veterinary Journal, 209, 201. http://dx.doi.org/10.1016/j.tvjl.2015.11.020

Mikolajczyk, J., Scott, F.L., Krajewski, S., Sutherlin, D.P., & Salvesen, G.S. (2004). Activation and substrate specificity of caspase-14. Biochemistry 43, 10560-10569. http://dx.doi.org/10.1021/bi0498048.

Nadiri, A., Wolinski, M.K., & Saleh, M. (2006). The inflammatory caspases : Key players in the host response to pathogenic invasion and sepsis. Journal of immunology 177, 4239-4245. http://dx.doi.org/10.4049/jimmunol.177.7.4239.

Nicholson, D.W., Ali, A., Thornberry, N.A., Vaillancourt, J.P., Ding, C.K., Gallant, M., & Lazebnik, Y.A. (1995). Identification and inhibition of the ICE/CED-3 protease necessary for mammalian apoptosis. Nature 376, 37-43. http://dx.doi.org/10.1038/376037a0.

Sadowski-Debbing, K., Coy, J.F., Mier, W., Hug, H., & Los, M. (2002). Caspases-their role in apoptosis and other physiological processes as revealed by knock-out studies. Archivum Immunologiae Et Therapiae Experimentalis 50, 19-34.

Sakamaki, K., & Satou, Y. (2009). Caspases: evolutionary

aspects of their functions in vertebrates. Journal of fish biology 74, 727-753. http://dx.doi.org/10.1111/j.1095-8649.2009.02184.x.

Seidelin, J.B., Strater, J., & Nielsen, O.H. (2013). Caspase 14 does not influence intestinal epithelial cell differentiation. Cell death and differentiation 20, 524. http://dx.doi.org/10.1038/cdd.2012.164.

Thornberry, N.A., Bull, H.G., Calaycay, J.R., Chapman, K.T., Howard, A.D., Kostura, M., & Aunins, J.G. (1992). A novel heterodimeric cysteine protease is required for interleukin-1 beta processing in monocytes. Nature 356, 768-774. http://dx.doi.org/10.1038/356768a0.

Van, D.C.M., Van, L.G., Pype.S., Van, C.W., Van, D.B.I., Molemans, F., ... Vandenabeele, P. (1998). Identification of a new caspase homologue: caspase-14. Cell death and differentiation, 5(10), 838. http://dx.doi.org/10.1038/sj.cdd.4400444.

Wang, L., Zhi, B., Wu, W., & Zhang, X. (2008). Requirement for shrimp caspase in apoptosis against virus infection. Developmental and comparative immunology 32, 706-715. http://dx.doi.org/10.1016/j.dci.2007.10.010.

Yamashita, N., Kannan, K., Taniyasu, S., Horii, Y., Okazawa, T., Petrick, G., & Gamo, T. (2004). Analysis of perfluorinated acids at parts-per-quadrillion levels in seawater using liquid chromatography-tandem mass spectrometry. Environmental Science & Technology 38, 5522-5528. http://dx.doi.org/doi//10.1021/es0492541.

Zhao, Z., Teng, Y., Liu, H., Lin, X., Wang, K., Jiang, Y., & Chen, H. (2007). Characterization of a late gene encoding for MCP in soft-shelled turtle iridovirus (STIV). Virus research 129, 135-144. http://dx.doi.org/10.1016/j.virusres.2007.07.002.

Zhou, J., Yang, X., & Ai, X. (1999). Pathogen of the furunculosis, red neck and red spot complicating diseases of *Trionyx sinensis*. Journal of Fisheries of China 23, 271-277. http://dx.doi.org/10.3321/j.issn:1000-0615.1999.03.010.

Zhou, X., Wang, L., Feng, H., Guo, Q., & Dai, H. (2011). Acute phase response in Chinese soft-shelled turtle (*Trionyx sinensis*) with *Aeromonas hydrophila* infection. Developmental and comparative immunology 35, 441-451. http://dx.doi.org/10.1016/j.dci.2010.11011.